

Fig. S1. Laminin subunits exhibit tissue-specific expression

A-F: Single z-plane confocal images of fluorescent mRNA *in situ* hybridization analysis of *lama4*, *lamb1b*, *lama5*, *lamb2*, *lamb1a* or *lamc1* expression (cyan) in *Tg(myl7:eGFP)* embryos (myocardium, green) counterstained for *fli1* mRNA (endocardium, magenta). *lama4* and *lamb1b* expression colocalises with *fli1* in the endocardium (A,B), while *lama5* and *lamb2* are expressed in the myocardium (C,D). *lamb1a* and *lamc1* are expressed in both myocardial and endocardial cells (E,F). Scale bars main panels: 50µm, insets: 10µm.

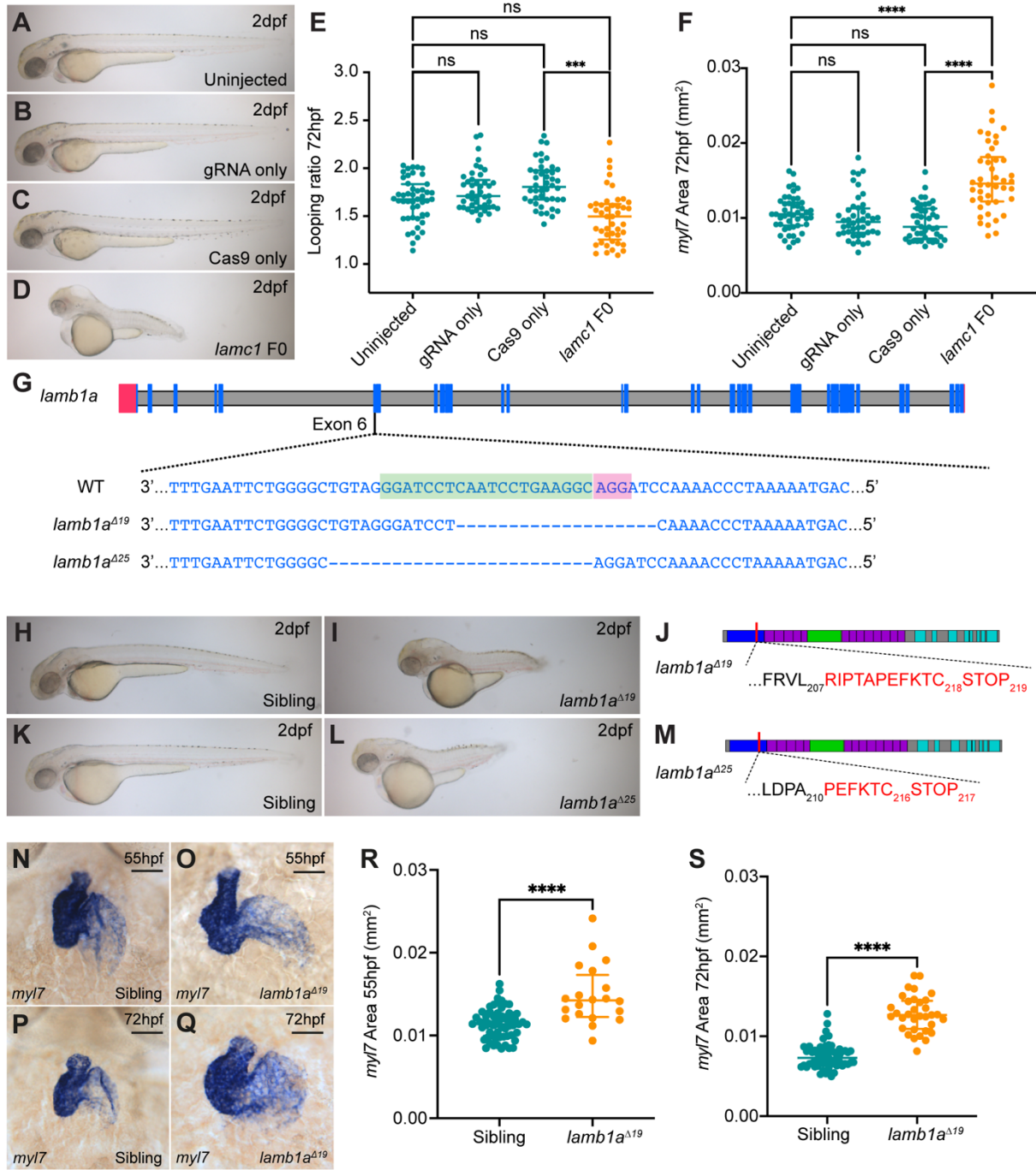


Fig. S2. *lamc1* and *lambla* mutants have defects in heart morphogenesis

A-D: Brightfield images of uninjected control (A), gRNA- or Cas9-only injected controls (B,C) or *lamc1* F0 crispant embryos (D) at 2dpf. Lateral views, anterior to left. E-F: Quantification of looping ratio (E) and heart size (F) in uninjected embryos (n=47), gRNA only control embryos (n=44), Cas9 only control embryos (n=44), and *lamc1* crispants (n=44) at 72hpf. Kruskal-Wallis test. G: Schematic depicting *lambla* gene (danRer10/GRCz10), with non-coding exons in red and coding exons in blue. gRNA target site (green) is located in exon 6 of wild type (WT) *lambla* (magenta indicates PAM sequence), and 2 deletion alleles of 19bp and 25bp were recovered. H-L: Brightfield images of sibling embryos (H,K), *lambla*^{A19} (I) and *lambla*^{A25} mutant embryos (L) and 2dpf. J,M: Schematic representation of Lamb1a protein structure (UniProt Q8JHV7), with the alterations in amino acid sequence depicted in red. Both *lambla* mutant alleles result in frameshift and insertion of a stop codon. N-Q: mRNA *in situ* hybridization analysis of *myl7* expression in sibling (N,P) and *lambla*^{A19} mutant embryos (O,Q) and 55hpf and 72hpf. Ventral views, anterior to top. R-S: Quantification of *myl7* area reveals a significant increase in heart size in *lambla* mutants (55hpf: n=20; 72hpf: n=33) when compared to siblings (55hpf: n=62; 72hpf: n=62) at 55hpf and 72hpf. Median +/- interquartile range. Mann-Whitney test. **** = p < 0.0001, *** = p < 0.001, ** = p < 0.01. Scale bars: 50µm.

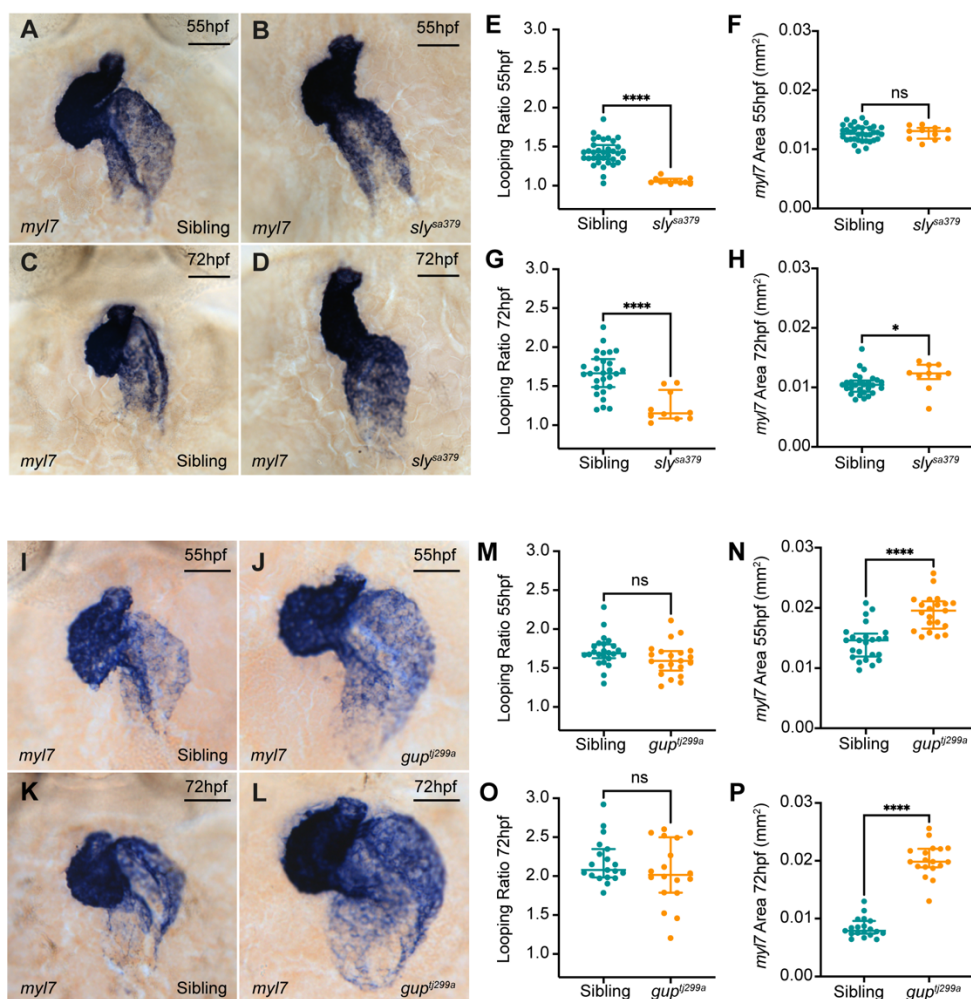


Fig. S3. *sleepy* and *grumpy* mutants recapitulate *lamc1* crispant and *lambla* mutant heart phenotypes

A-D: mRNA *in situ* hybridization analysis of *myl7* expression in sibling (A: n=35; C: n=28) and *sly^{sa379}* mutant embryos (B: n=11; D: n=10) at 55hpf and 72hpf. Ventral views, anterior to top. E-H: Quantification of looping ratio in sibling and *sly^{sa379}* mutant embryos reveals a reduction in heart looping morphology at both 55hpf (E) and 72hpf (G). Heart size is unaffected in *sly^{sa379}* mutant embryos compared to siblings at 55hpf (F), however *sly^{sa379}* mutants have slightly enlarged hearts at 72hpf (H). I-L: mRNA *in situ* hybridization analysis of *myl7* expression in sibling (I: n=24; K: n=19) and *gup^{tj299a}* mutant embryos (J: n=21; L: n=18) at 55hpf and 72hpf. Ventral views, anterior to top. M-P: Quantification of looping ratio reveals no significant difference in looping morphology between sibling and *gup^{tj299a}* mutant embryos (M,O). However, *gup^{tj299a}* mutant embryos exhibit enlarged hearts when compared to siblings at both 55hpf (N), and 72hpf (P). Median +/- interquartile range. Mann-Whitney test, **** = $p < 0.0001$, *** = $p < 0.001$, ** = $p < 0.01$, * = $p < 0.05$, ns = not significant. Scale bars: 50 μm.

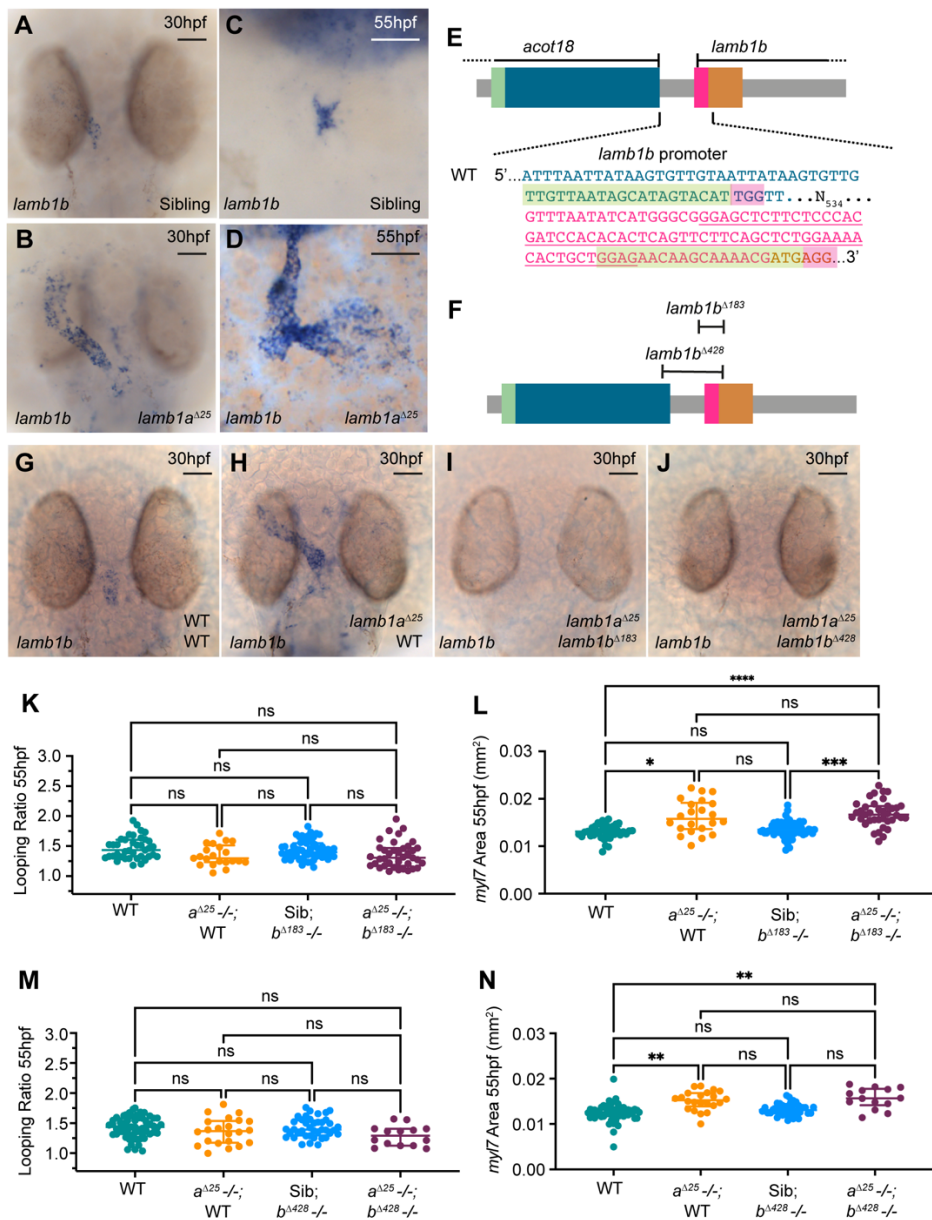


Fig. S4. *lamb1b* is dispensable for heart development

A-D: mRNA *in situ* hybridization expression analysis of *lamb1b* in sibling (A,C) and *lamb1a*^{A25} mutant embryos (B,D) at 30hpf and 55hpf. *lamb1a*^{A25} mutants exhibit an upregulation of *lamb1b* throughout the endocardium (30hpf: n=15/16; 55hpf: n=13/14) compared to wild types (30hpf: n=15/17; 55hpf: n=12/13) at both stages. A-B: Dorsal views, anterior to top; C-D: Ventral views, anterior to top. E-F: Schematic representation of CRISPR gRNAs (green sequence, PAM in magenta) targeting the promoter of *lamb1b* (danRer10/GRCz10). Two *lamb1b* deletion alleles were recovered: *lamb1b*^{A183} and *lamb1b*^{A428}. G-J: mRNA *in situ* hybridization analysis of *lamb1b* expression in wild type (G), *lamb1a*^{A25} mutants (H), *lamb1b*^{A183};*lamb1a*^{A25} double mutants (I), or *lamb1b*^{A428};*lamb1a*^{A25} double mutants (J). *lamb1b* expression is abrogated in both *lamb1b*^{A183};*lamb1a*^{A25} (n=6/6) and *lamb1b*^{A428};*lamb1a*^{A25} double mutants (n=6/6) (I,J). Dorsal views, anterior to top. K-L: Quantification of heart looping ratio (K) and *myl7* expression domain as a proxy for heart size (L) in wild type (n=39), *lamb1a*^{A25} single mutants (n=22), *lamb1b*^{A183} single mutants (n=62), and *lamb1b*^{A183};*lamb1a*^{A25} double mutant embryos (n=39) at 55hpf. M,N: Quantification of heart looping ratio (M) and heart size (N) in wild type (n=60), *lamb1a*^{A25} single mutants (n=22), *lamb1b*^{A428} single mutants (n=40), and *lamb1b*^{A428};*lamb1a*^{A25} double mutant embryos (n=14) at 55hpf. Loss of *lamb1b* in *lamb1a*^{A25} neither induces defects in heart looping morphology, nor rescues heart size, in *lamb1a*^{A25} mutants. Median +/- interquartile range. Kruskal Wallis test, * = p < 0.05, ns = not significant. Scale bars: 50µm.

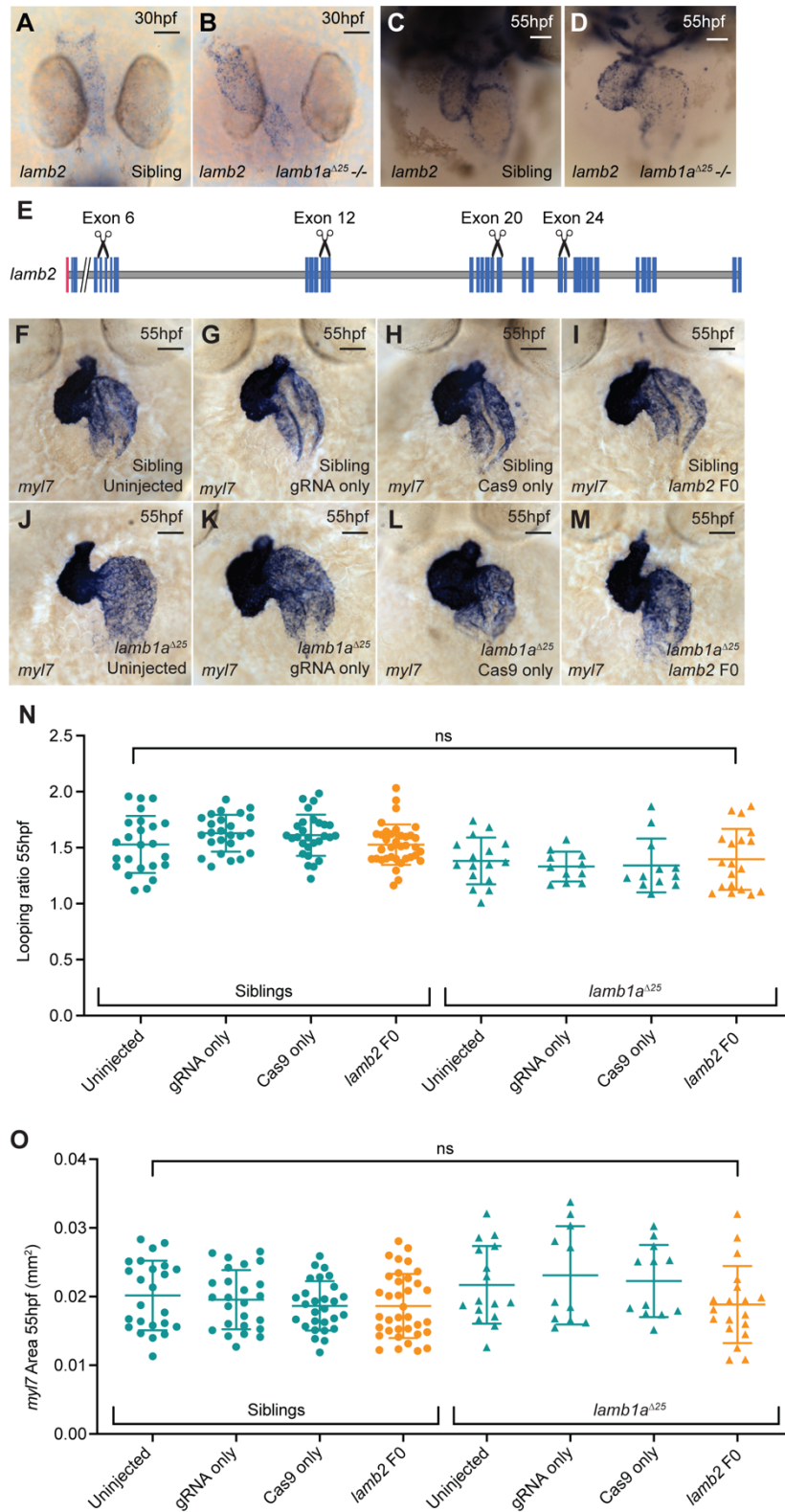


Fig. S5. *lamb2* does not compensate for loss of *lamb1a* in the developing heart A-D: mRNA *in situ* hybridization expression analysis of *lamb2* expression in the heart of sibling (A,C) and *lamb1a*^{A25} mutants (B,D) at 30hpf and 55hpf. At both 30hpf and 55hpf *lamb2* expression in *lamb1a*^{A25} mutants (B: 30hpf, n= 16/20; D: 55hpf, n=13/15) is comparable when compared to siblings (A: 30hpf, n=10/13; C: 55hpf, n=15/15). E: Schematic depicting *lamb2* gene (danRer10/GRCz10), with non-coding exons in red and coding exons in blue. 4 CRISPR gRNA target sites (scissors) were selected throughout the gene. F-M: mRNA *in situ* hybridization analysis of *myl7* expression at 55hpf in sibling and *lamb1a*^{A25} mutant embryos, either uninjected controls (F,J), controls injected with *lamb2*-targeting gRNAs only (G,K), controls injected with Cas9 protein only (H,L), or experimental samples with *lamb2*-targeting gRNAs together with Cas9 protein (*lamb2* F0, I,M). N-O: Quantitative analysis of looping ratio (N) and *myl7* area (O) at 55hpf in uninjected controls (siblings n=24, *lamb1a*^{A25} mutants n=16), gRNA-injected controls (siblings n=25, *lamb1a*^{A25} mutants n=11), Cas9-injected controls (siblings n=28, *lamb1a*^{A25} mutants n=12) and *lamb2* F0 crispants (siblings n=36, *lamb1a*^{A25} mutants n=19). No significant differences are observed between any experimental groups, indicating CRISPR-mediated mutagenesis of *lamb2* does not alter the *lamb1a* mutant phenotype. Median +/- interquartile range, Kruskal-Wallis test, ns = not significant.

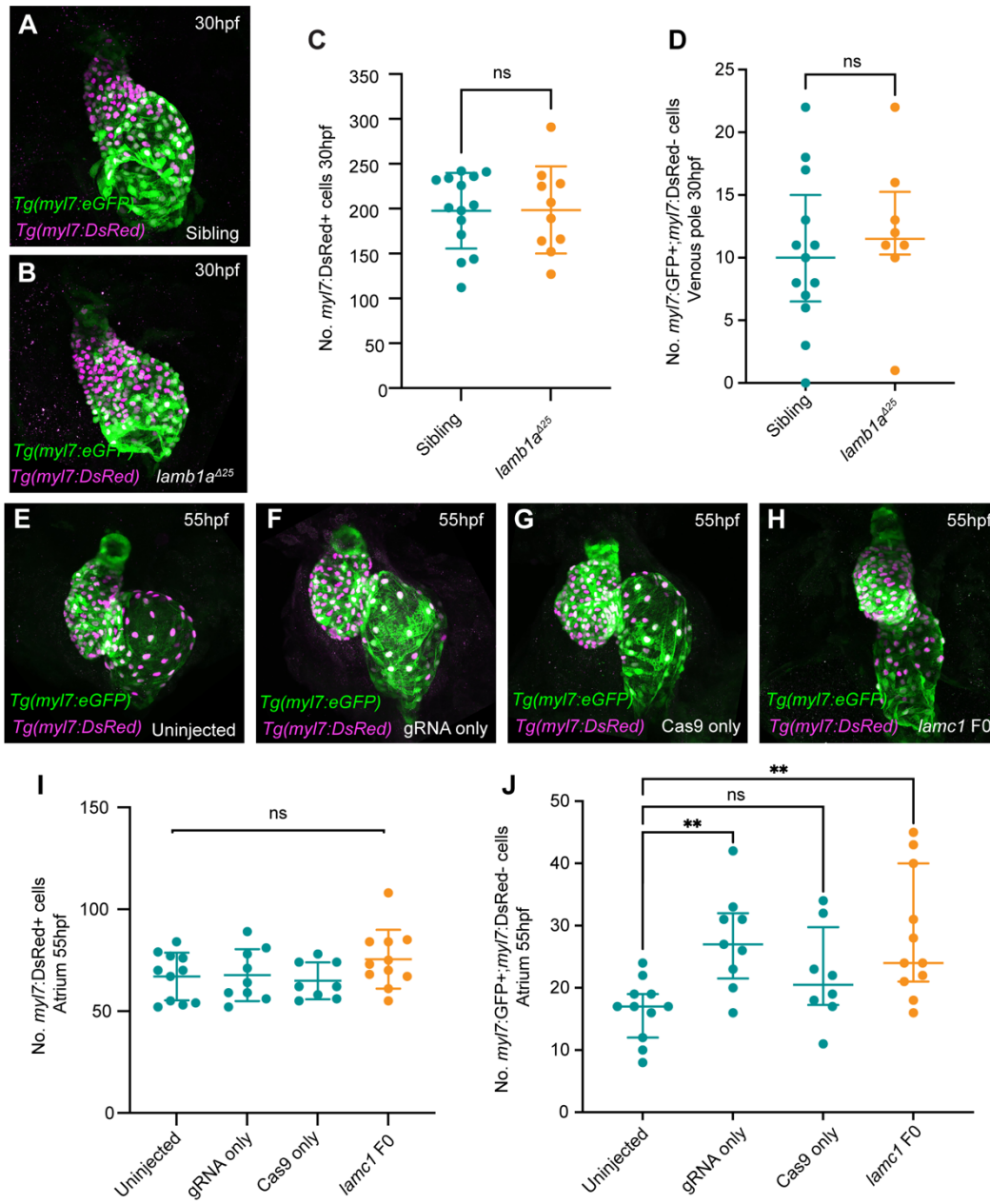


Fig. S6. Laminin restricts SHF addition during looping morphogenesis

A-B: Maximum intensity projections of confocal image z-stacks in *Tg(myl7:eGFP);Tg(myl7:DsRed)* double transgenic sibling (A) and *lambl α ^{A25}* mutant embryos (B) at 30hpf. C: Quantification of GFP+ DsRed+ cell number in the heart tube of sibling (n=14) and *lambl α ^{A25}* mutant embryos (n=10) at 30hpf reveals no significant difference in the number of dsRed+ cardiomyocytes. D: Quantification of GFP+;DsRed- SHF cell number in siblings (n=13) and *lambl α ^{A25}* mutants (n=8) at 30hpf reveals no change in newly-added SHF cells in *lambl α ^{A25}* mutants compared to siblings. E-H: Maximum intensity projections of confocal image z-stacks in *Tg(myl7:eGFP);Tg(myl7:DsRed)* double transgenic uninjected control (E), gRNA only injected controls (F), Cas9 only controls (G), and *lamc1* crispants (H) at 55hpf. I: Quantification of GFP+;DsRed+ cell number in the atrium of uninjected controls (n=11), gRNA only injected controls (n=9), Cas9 only injected controls (n=8) and *lamc1* F0 crispant embryos (n=11) at 55hpf. No significant differences in DsRed+ cell number in *lamc1* F0 crispants were observed. J: Quantification of GFP+;DsRed- SHF cell number at the venous pole in uninjected controls (n=11), gRNA only injected controls (n=9), Cas9 only injected controls (n=8) and *lamc1* F0 crispant embryos (n=11) at 55hpf reveals a significant increase in newly-added SHF cells to the venous pole in *lamc1* crispants when compared to uninjected controls. Horizontal bars indicate mean \pm s.d, C,D: Mann-Whitney test. I: Kruskal Wallis test. J: Brown-Forsythe and Welch ANOVA test, ** = $p < 0.01$, ns = not significant. Scale bars: 50 μ m.

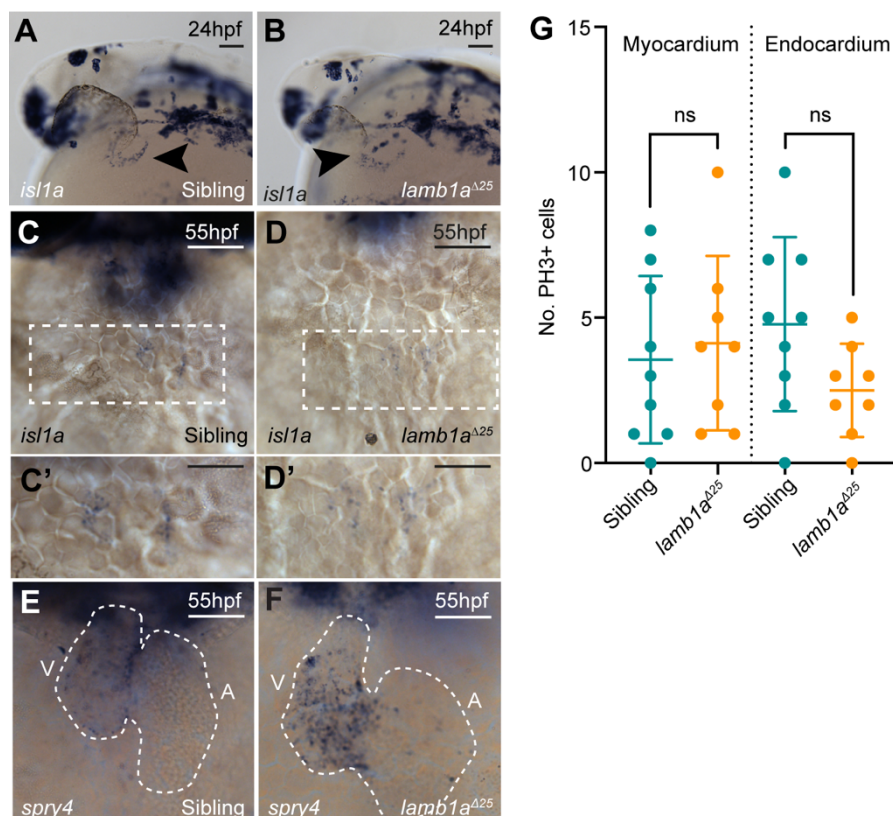


Fig. S7. *isll1* expression is unaffected and *spry4* is upregulated in *lamb1a* mutant embryos

A-D: mRNA *in situ* hybridization analysis of *isll1* expression at 24hpf (A,B) and 55hpf (C,D) in sibling and *lamb1a*^{A25} mutant embryos. The domain of *isll1* expression at the venous pole of the heart (black arrowhead) is unaffected in *lamb1a*^{A25} mutants (B, n=22/28; D, n=17/23) when compared to sibling embryos (A, n=23/29; C, n=38/47) at both stages. C',D': Higher magnification of venous pole region contained in white box in C and D. E-F: mRNA *in situ* hybridization analysis of *spry4* expression at 55hpf reveals a mild upregulation of *spry4* expression in *lamb1a*^{A25} mutants (F, n=10/21) when compared to siblings (E, n=48). G: Quantification of PH3-positive proliferation cells in the myocardium and endocardium of sibling (n=9) and *lamb1a*^{A25} mutant embryos (n=8) at 55hpf. There is no significant difference in proliferation upon loss of *lamb1a*. Mean \pm s.d., unpaired t test. Scale bars: 50 μ m.

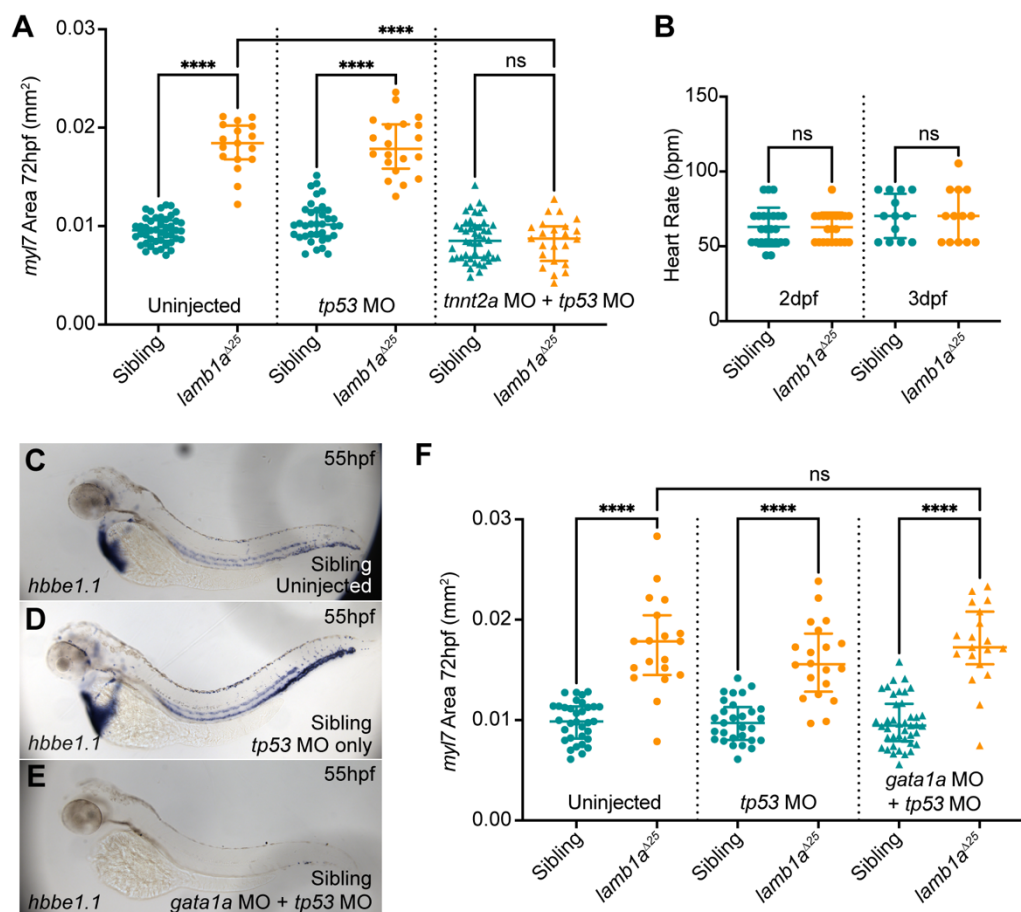


Fig. S8. Lamb1a restricts cardiac growth independent of haemodynamic force A: Quantification of *myl7* expression domain at 72hpf as a proxy for heart size in sibling and *lamb1a*^{Δ25} mutants, either uninjected (sibling: n=45; *lamb1a*^{Δ25} mutants: n=17), injected with *tp53* MO (sibling: n=36; *lamb1a*^{Δ25} mutant: n=20) or co-injected with *tp53* MO and *tnnt2a* MO (sibling: n=46; *lamb1a*^{Δ25} mutant: n=23). Cardiomegaly is rescued in *lamb1a*^{Δ25} mutants injected with *tnnt2a* MO. B: Quantification of heart rate in sibling and *lamb1a*^{Δ25} mutant embryos at 2dpf and 3dpf reveals that *lamb1a*^{Δ25} mutants do not exhibit an elevated heart rate. C-D: mRNA *in situ* hybridization analysis of *hbbe1.1* expression at 55hpf in sibling embryos, either uninjected (C), *tp53* MO (D), or *tp53* MO and *gata1a* MO (E). Injection of *gata1a* MO prevents the formation of erythroid cells (E). Lateral views, anterior to left. F: Quantification of *myl7* expression domain as a proxy for heart size in sibling and *lamb1a*^{Δ25} mutants, either uninjected (sibling: n=33; *lamb1a*^{Δ25} mutants: n=19), injected with *tp53* MO (sibling: n=29; *lamb1a*^{Δ25} mutant: n=20) or co-injected with *tp53* MO and *gata1a* MO (sibling: n=41; *lamb1a*^{Δ25} mutant: n=19) reveals that loss of erythroid cells through injection of *gata1a* MO does not rescue heart size in *lamb1a*^{Δ25} mutant embryos. All statistical analyses performed using Mann-Whitney test, **** = $p < 0.0001$, ns = not significant. Scale bars: 50 μ m.

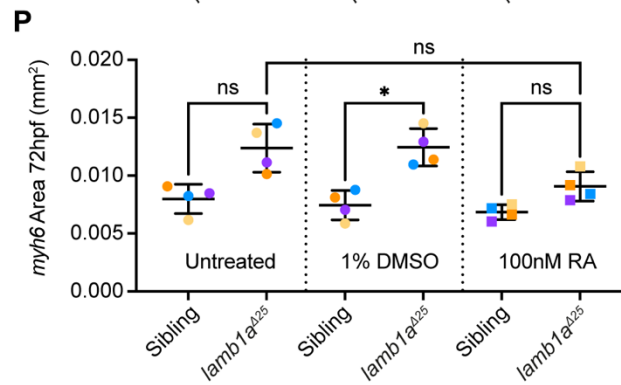
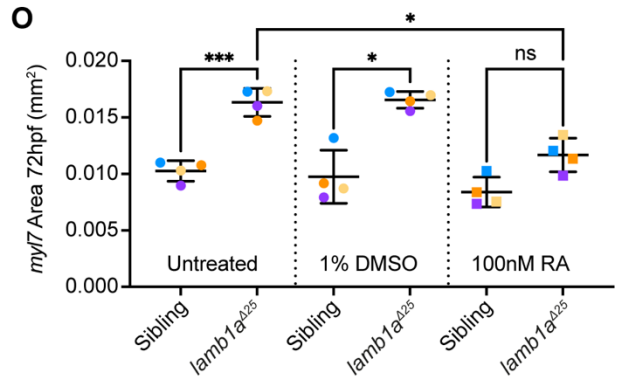
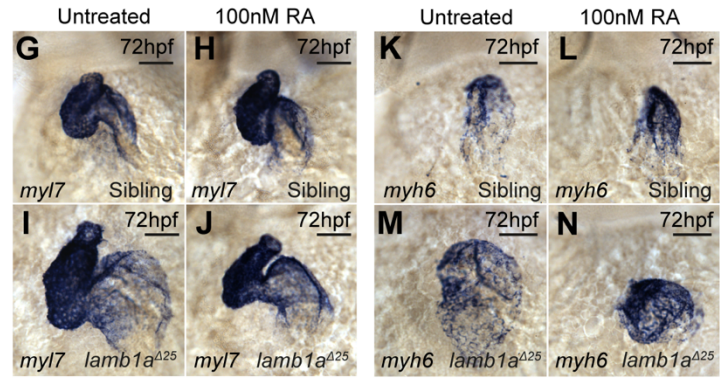
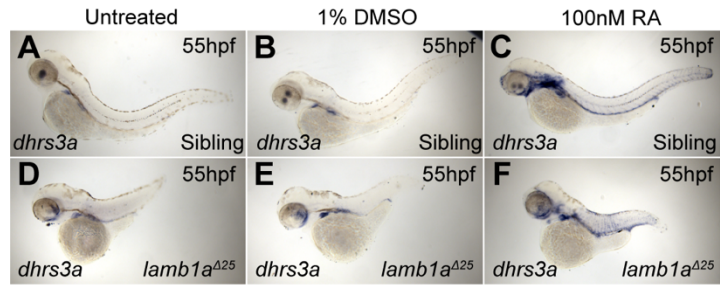


Fig. S9. Retinoic Acid treatment during SHF addition partially rescues cardiomegaly in *lambla* mutant embryos

A-F: mRNA *in situ* hybridization analysis of *dhrs3a* expression at 55hpf in sibling and *lambla*^{A25} mutants either untreated, incubated with DMSO, or incubated with 100nM RA from 24hpf to 55hpf. RA treatment results in an upregulation of the RA-responsive gene *dhrs3a* (C, F) compared to untreated controls (A,B,D,E). Lateral views, anterior to left). G-J: mRNA *in situ* hybridization expression analysis of *myl7* expression at 72hpf in sibling and *lambla*^{A25} mutant embryos, either untreated (G,I) or incubated in 100nM RA between 24hpf and 55hpf (H,J). K,N: mRNA *in situ* hybridization expression analysis of *myh6* at 72hpf in the atrium of sibling and *lambla*^{A25} mutant embryos, either untreated (K,M) or incubated in 100nM RA between 24hpf and 55hpf (L,N). Ventral views, anterior to top. O-P: Quantification of *myl7* expression domain (O) and *myh6* expression domain (P) in control and RA-treated embryos. RA treatment significantly reduces heart size in *lambla* mutants compared to controls (O). Median +/- interquartile range. All statistical analyses performed using Kruskal Wallis test, *** = $p < 0.001$, * = $p < 0.05$, ns = not significant. Scale bars: 50 μ m.

Table S1. primers and gene sequences used to generate novel in situ mRNA probes

Probe	Primer Sequence	Accession Number; ZFIN ID
<i>lama4</i>	F: 5'-CGATCAACTGCAGAGACACG-3'	ENSDARG00000020785; ZDB-GENE-040724-213
	R: 5'-GATGAACTTCTGCTCGGCTG-3'	
<i>lama5</i>	F: 5'-CCCTCGCACCAATACATGTG-3'	ENSDARG00000058543; ZDB-GENE-030131-9823
	R: 5'-CATTGGGTCTGCATCGACAG-3'	
<i>lamb1a</i>	F: 5'-TCCAATTACCCACCTCATC-3'	ENSDARG00000101209; ZDB-GENE-021226-1
	R: 5'-GGTCACAGTTCCTTCCGGTA-3'	
<i>lamb2</i>	F: 5'-CAAGACAACCGAAGCCAACA-3'	ENSDARG00000002084; ZDB-GENE-081030-4
	R: 5'-GGCTTACAGTCAGGGAAGGT-3'	
<i>lamc1</i>	F: 5'-GTGCTCTTGTAATCCAGCCG-3'	ENSDARG00000036279; ZDB-GENE-021226-3
	R: 5'-GCTCACATCGCTTACCTGTG-3'	
<i>islla</i>	F: 5'-GGACCTAACACCGCCTTACT-3'	ENSDARG00000004023; ZDB-GENE-980526-112
	R: 5'-TAGGACTCGCTACCATGCTG-3'	
<i>dhrs3a</i>	F: 5'-AAAGGTGATTTTGTGGGGCC-3'	ENSDARG00000044982; ZDB-GENE-040801-217
	R: 5'-AACAAGCCATCTCGATTCGC-3'	